Determination of salinity gradient power potential in Québec, Canada

Y. Berrouche[a)] and P. Pillay
Department of Electrical and Computer Engineering, Concordia University, Québec H3G 1M8, Canada

(Received 24 March 2012; accepted 7 September 2012; published online 4 October 2012)

Electrical energy can be produced from the chemical potential difference of two liquids with dissimilar salinities. This source of energy is known as salinity gradient power. In this paper, the theory, the technologies used to exploit the power, the major challenges, and their development trends are first presented. Then a modeling of fluxes across semi permeable membranes is proposed and validated. Next, an energy balance study is done in order to estimate the power potential for a given salinity gradient system. By applying this study to several rivers in Quebec, the salinity power gradient potential is estimated to 45 TWh/yr based on the minimal flow rate of each river. © *2012 American Institute of Physics*. [http://dx.doi.org/10.1063/1.4754439]

I. INTRODUCTION

In the power generation field, there is a tendency to increase the use of renewable energy sources, such as wind, solar, marine, and biomass.[1] Various sources can be used to produce marine energy, such as tides, ocean currents, and salinity gradient. It has been demonstrated that the salinity gradient represents a high energy density compared to other marine energy sources.[2] A difference in the chemical potential which is available when fresh water (River) meets salt water like the ocean, sea, gulf, or saline lake can be exploited to produce electricity.[6] In Ref. 3, it is shown that the salinity gradient power (SGP) can fulfill 7% of the world's total energy needs.

Many technologies have been developed to exploit the salinity gradient power, such as pressure retarded osmosis (PRO), reversed electrodialysis (RED), hydrocratic generator,[4] and vapor compression.[5] These technologies are under research and development, but the technologies that can be commercialized are only the RED and PRO. In the PRO technology, the salt water meets fresh water via a semi-permeable membrane. By the phenomenon of osmosis, the fresh water flows through the membrane to the side of the salt water, thus increasing the pressure on this side. This hydraulic power can be transformed to electrical power using a turbine and generator. In RED technology, the inverse phenomenon of electrodialysis (using anion and cation exchange membranes) is used to produce DC power.

A. Pressure retarded osmosis

This technology was first recognized by Sidney Loeb.[6–10] In 1950s, Loeb designed a system that produces drinking water from the seawater using a high pressure pump. Nowadays, his system is being used in desalination stations. In 1975, he patented his system which can be used in reverse in order to produce energy, which he called pressure retarded osmosis.

The working principal of the PRO is presented in Fig. 1. Basically, the system requires two water chambers separated by a semipermeable membrane, pressure exchanger, turbine, filters, pumps, and generator. Fresh water is first pumped into a chamber by a pump, where the

[a)]Author to whom correspondence should be addressed. Electronic mail: yberrouche@gmail.com.

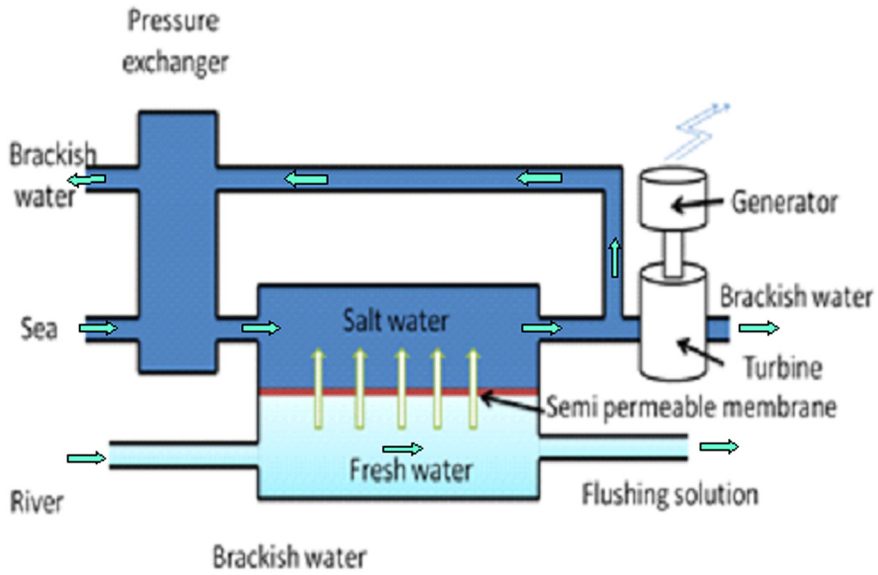

FIG. 1. Principal of the pressure retarded osmosis.

pressure is less than the osmotic pressure between the fresh and the salt water. About 90% of this fresh water flows to the salt water chamber through the semipermeable membrane, increasing the pressure in the salt water chamber.[10] The water at high pressure will be divided into two portions: one portion flows through the turbine that drives the generator and the other portion is returned to the pressure exchanger that recycles the energy and adds pressure to the system from Refs. 6–10.

In 1970s, the semi-permeable membrane was not fully developed and its cost was very high.[8,9] After an economic study carried out by Loeb, it was concluded that the price per Watt for energy production using sea and fresh waters is excessive. So he considered a lake with a high concentration of salt such as the Dead Sea in Jordan.[8] The salinity of the Dead Sea is about 120 PSU (practical salinity unit), which is much higher than that of regular sea or ocean water (35 PSU). Therefore, it provides more power for a lower price.

He considered an analysis on a 66 MW hydroelectric power plant at the Great Salt Lake in Jordan with capital costs of $9000 per kW. The calculated energy price would be $0.09/kWh.[9] The energy price will mainly depend on the ability to attain adequate permeate flux through the membrane. Due to the low efficiency of the membrane at that time, the semipermeable membrane will be easily oxidized by the high salinity of the water.

In 1997, the PRO was revived by the Norwegian Foundation for Scientific and Industrial Research (SINTEF). After making many laboratory tests on the PRO, the SINTEF announced that the membrane technology has been developed enough to be used in real power generation plants.[11,12] The results analyzed by SINTEF were transferred to Statkraft that adopted the PRO technology to become the first worldwide leader in this area. Statkraft being the largest renewable energy company in Europe opened the first laboratory that focuses on salinity gradient power. Statkraft believed that the research should be focused on the membrane technology in order to increase its efficiency and therefore reduce the cost of power production. For that, several collaborations have been developed between Statkraft and industrial and academic research centers specialized in membrane technologies located in Germany, Netherlands, and Norway. A remarkable improvement has been realized; the annual report published by Statkraft in 2009 shows that their membrane generates 3 W/m^2, while their first generation (1999) generated only 0.1 W/m^2. The goal of this research was to target 5 W/m^2.[13]

In October 2009, Statkraft launched the first worldwide osmotic power prototype plant in Tofte in Norway. This plant would have a limited production capacity (4 kW) and is primarily intended for testing and development purposes. The aim is to be able to construct a commercial

osmotic power plant before 2015. This will be the size of a football stadium, containing 5×10^6 m^2 of membrane and generation capacity of 25 MW of electricity. Statkraft estimates that the Norway potential salinity gradient power is about 12 TWh/yr and that of the whole world is 1600 to 1700 TWh which is equal to the China's total electricity consumption in 2002.[13]

B. Reversed electrodialysis (blue energy)

The Netherlands Company Wetsus is developing another technology that uses inverse electrodialysis to produce energy from water salinity gradients. They named it Blue Energy. Wetsus thinks that the rivers in the Netherlands unlike in Norway contains a lot of deposits and bacteria and the cost of filtering this water will be high enough to make the PRO uncommercial. The operating principle of the blue energy is presented in Fig. 2.

The RED technology needs anion exchange membranes, cation exchange membranes, electrodes, and pumps. The anion and cation exchange membranes are put in alternate layers in order to create chambers. When the fresh water and seawater flow simultaneously, chlorine ions flow to the electrode through the anion exchange membranes but blocked by the cation exchange membrane and vice versa for the sodium ions. The motion of these ions creates an internal electrical current and therefore a DC voltage.[3,14–17]

After doing laboratory tests on a 20 W prototype developed by Wetsus,[19] the Dutch company Magneto formed a new company called Redstack to collaborate with Wetsus in order to commercialize the RED technology.[20] Both companies are piloting together a RED project in Harlingen that produces several kilowatts. This company estimates that the blue energy could provide up to 7% of the global energy needs by exploiting half of worldwide rivers flow. Redstack is developing a new plant in the lake IJsselmeer of the Netherlands. This 200 MW plant will cost $600 million for construction. As a comparison between the two plants, the produced energy costs $90/MW h for the RED technology in Ijsselmeer and between $65 and $125 for the PRO technology in Tofte.[13]

Both technologies are in the same stage of development and both groups are working in competition to prove that their technology is the best for exploiting the Gradient Salt energy. This new source of renewable energy is applicable not only in Norway and the Netherlands but in the whole world including Québec.

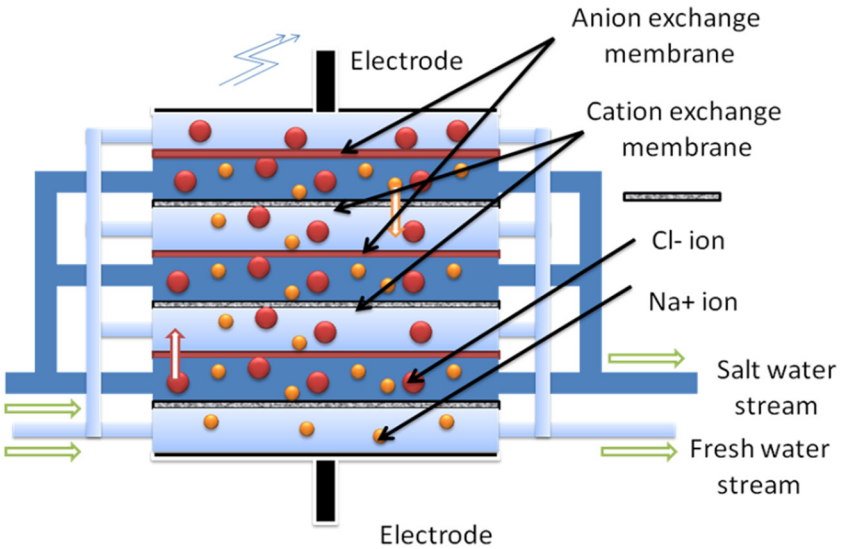

FIG. 2. Principal of the reversed electrodialysis.

II. SGP POTENTIAL IN QUÉBEC

Québec has a target of 20% reduction of CO_2 emissions for 2020.[10] In 2005, hydrocarbon emissions in Québec amounted to 66 Mtons or 71.7% of total CO_2 emissions. The transportation sector was responsible for 53.9% of this volume, while mining and manufacturing accounted for 19.3%, residential, commercial, and institutional sub-sectors 18.2%, and energy distribution, transport, and production 7.7%.[21]

In the 2006-2012 Action Plan on Climate Change (APCC), the Government of Québec unveiled its energy strategy, entitled Using Energy to Build the Québec of Tomorrow. This strategy foresees new developments in renewable energy (hydroelectricity, wind energy, and biomass) and seeks a more efficient utilization of all forms of energy.[1,21]

In order to estimate the electrical power that can be generated from a gradient in salinity, it is required to develop an analytical formula of the produced power. This formula depends on the type of technology used. In this paper, the PRO technology is selected in order to estimate the electrical power that can be produced in Québec.

A. Flux modeling across semipermeable membrane

1. The salt diffusion equation

Consider a solution containing solute (salt) dissolved in solvent (water) like seawater. At the microscopic level, the salt molecules are moving under diffusion which is their thermal motion at temperatures above absolute zero. The rate of this movement is a function of temperature, viscosity of the fluid, and the size (mass) of the salt particles. This motion can be expressed by Fick's first low that relates the diffusive flux to the concentration field, by postulating that the flux goes from regions of high concentration to regions of low concentration, with a magnitude that is proportional to the concentration gradient[22,23]

$$J_S = -D\frac{dC}{dx}. \tag{1}$$

In Eq. (1), Js, D, C, and x are the salt diffusive flux (mol m^{-2} s^{-1}), the coefficient of diffusion (m^2 s^{-1}), the salt concentration (mol m^{-1}), and the linear coordinate (m), respectively. The diffusion constant D can be estimated by Stokes-Einstein equation as[24]

$$D = \frac{k_B \cdot T}{6.\pi \cdot \mu \cdot r}, \tag{2}$$

where kB is Boltzmann's constant (1.38×10^{-23} m^2 kg s^{-2} K^{-1}), μ is the viscosity (Pa s), r is the radius of the diffused particles (m), and T is the temperature (K).

Fick's second law can be generated for space coordinates as

$$\frac{\partial C}{\partial t} = \nabla \cdot (D \cdot \nabla C). \tag{3}$$

The total equation of the salt motion is given by coupling the diffusion with the convection of the salt

$$\frac{\partial C}{\partial t} - \nabla \cdot (D \cdot \nabla C) + \vec{V} \cdot \nabla \vec{C} = 0, \tag{4}$$

where $\vec{V}$ is liquid velocity vector.

2. Osmosis for ideal case

If a semipermeable membrane is used to separate this solute with pure water; the salt will have a tendency to diffuse from the high concentration side to the low concentration side. This

salt will be blocked at the membrane and a hydraulic pressure will be created between the two sides of membrane; this pressure is called the osmotic pressure and it can be given by Van't Hoff law as

$$\Delta\Gamma \approx i \cdot R_g \cdot T \cdot \Delta C_S = K \cdot \Delta C_S, \tag{5}$$

where $\Delta\Gamma$, i, ΔC_S, R, T are the osmotic pressure difference (Pa), the Van't Hoff coefficient (equals to 2 for NaCl solution), the salt concentration (mol m^{-3}) between the membrane surfaces, the gas constant (8.314472 J mol^{-1} K^{-1}), and the temperature, respectively.

This osmotic pressure causes the water motion from the low to the high concentration side. This water flux can be given as

$$J_W = A \cdot (\Delta\Gamma - \Delta P). \tag{6}$$

In Eq. (6), J_w, A, and ΔP are the water flux (m^3 s^{-1} m^{-2}), water permeate flux coefficient (m s^{-1} Pa), and hydraulic (operating) pressure difference (Pa), respectively.

The performance of a PRO plant is essentially characterized by the specific power (W m^{-2}) which is the produced power per surface area of the membrane that can be given as

$$W_S = J_W \cdot \Delta P. \tag{7}$$

3. Osmosis for real case

In reality, there is no perfect membrane that blocks all the salt; there is always a small amount of salt that moves through the membrane. This salt permeate flux can be written as

$$J_S = B \cdot \Delta C_S, \tag{8}$$

where B is the salt permeate coefficient of the membrane (m s^{-1}).

The semi-permeable membrane is a very thin layer (few microns) that should be fixed to a porous support which has a thickness of about 100 μm. The membrane side is called the active layer. In the PRO case, the water and salt have an opposite sense results in an exponential distribution of the salt, which is called the concentration polarization phenomenon.

In Fig. 3, C_1 is the salt concentration in the bulk of the freshwater, C_2 is the salt concentration at the interface between the fresh water and the membrane support, C_3 is the salt concentration at the interface between the membrane support and the membrane skin, C_4 is the salt concentration at the surface of the membrane skin, while C_5 is the salt concentration in the bulk of the salt water.[27]

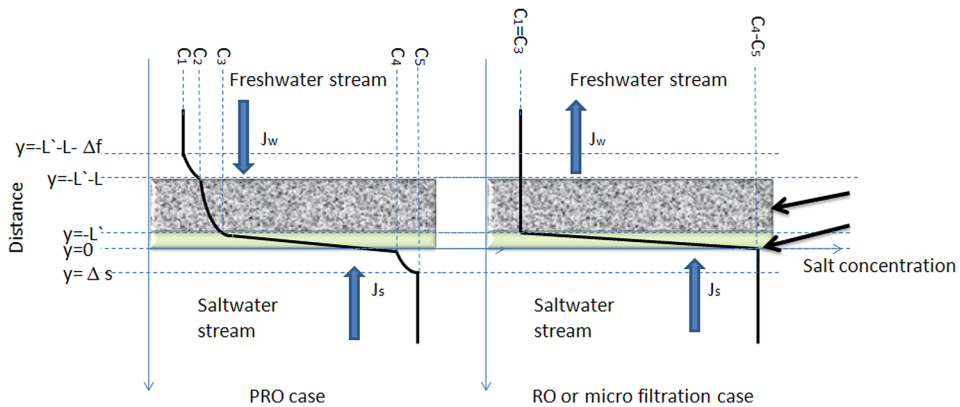

FIG. 3. Water and salt flux in osmosis reversed (OR) and PRO cases.

The porous support of the membrane is characterized by its porosity (Ψ), tortuosity (τ), and the effective length L_0 (m). The porosity represents the vacuum volume over the total volume occupied by the porous material. The tortuosity is given by the effective length of the porous medium over its real length (L)

$$\tau = \left(\frac{L_0}{L}\right)^2. \tag{9}$$

The structure parameter (m) of the porous support is given as

$$S = \frac{\tau L}{\psi}. \tag{10}$$

It has been demonstrated that the water flux and the linear cordinate inside the porous material can be given as[18]

$$V_p = J_{W.}\frac{\sqrt{\tau}}{\psi}, \tag{11}$$

$$y_P = \sqrt{\tau}\cdot y. \tag{12}$$

4. Equation of concentration

Assuming that the diffusion constant (D) does not vary with the geometry, the equation of the concentration given by Eq. (4) becomes

$$\frac{\partial C}{\partial t} = D\cdot\left(\frac{\partial^2 C}{\partial x^2}+\frac{\partial^2 C}{\partial y^2}+\frac{\partial^2 C}{\partial z^2}\right) - \begin{pmatrix} V_x \\ V_y \\ V_z \end{pmatrix}\cdot\left(\frac{\partial C}{\partial x},\frac{\partial C}{\partial y},\frac{\partial C}{\partial z}\right), \tag{13}$$

where V_x, V_y, and V_z are the cartesian coordinates of the water velocity vector.

For the steady sate case, Eq. (13) can be written in one dimension as

$$D\cdot\frac{\partial C}{\partial y} - J_W\cdot C = B\cdot\Delta C_S. \tag{14}$$

Physically, it can be seen that the net salt transport is equal to the salt diffusion minus the salt concentration coupled to the osmotic water flux in the opposite direction.

At the porous medium, Eq. (13) can be written as

$$D\cdot\frac{\partial^2 C}{\partial {y_p}^2} - V_P\cdot\frac{\partial C}{\partial y_p} = 0. \tag{15}$$

By introducing Eqs. (11) and (12) in Eq. (15), this equation becomes

$$D\frac{\Psi}{\tau}\cdot\frac{\partial^2 C}{\partial y^2} - J_w\cdot\frac{\partial C}{\partial y} = 0. \tag{16}$$

Therefore,

$$\frac{dC}{dy} = \frac{\tau\cdot J_W}{\psi\cdot D}C + \frac{\tau\cdot B}{\psi\cdot D}\Delta C_S. \tag{17}$$

On the outside of the porous medium, Eq. (14) is written as

$$\frac{dC}{dy} = \frac{J_W}{D}C + \frac{B}{D}\Delta C_S. \tag{18}$$

Taking into account the boundary conditions represented in Fig. 3, the solution of Eqs. (17) and (18) is given as

$$C_2 = \left(C_1 + \frac{J_S}{J_W}\right) \cdot e^{\frac{J_W \Delta f}{D}} - \frac{J_S}{J_W}, \tag{19}$$

$$C_3 = \left(C_1 + \frac{J_S}{J_W}\right) \cdot e^{\frac{J_W (S+\Delta f)}{D}} - \frac{J_S}{J_W}, \tag{20}$$

$$C_4 = \left(C_5 + \frac{J_S}{J_W}\right) \cdot e^{\frac{-J_W \Delta s}{D}} - \frac{J_S}{J_W}, \tag{21}$$

where Δf and Δs are the film thickness of the fresh water side and the seawater side, respectively.

The salt concentration gradient can be deduced from Eqs. (8), (20), and (21) as

$$\Delta C_S = \frac{C_5 \cdot e^{-\frac{J_W \cdot \Delta s}{D}} - C_1 \cdot e^{\frac{J_W \cdot (\Delta f + S)}{D}}}{1 + \frac{B}{J_W} \cdot e^{\frac{J_W \cdot (\Delta f + S)}{D}} - \frac{B}{J_W} \cdot e^{-\frac{J_W \cdot \Delta s}{D}}}. \tag{22}$$

This system contains non linear equations and it cannot be solved analytically. Solving by iteration is proposed.

It can be seen from Eq. (22) that the salt concentration gradient can be determined as function of the known variables, such as the salt concentrations (C_5 and C_1), the salt permeate coefficient (B), and the diffusion coefficients (D). In addition to this, Eq. (22) depends non-linearly on the water flux (J_w) which is related to the pressure by Eq. (6). This system cannot be solved analytically; a numerical solution is required in order to determine the concentration gradient. The flow chart of this solution is presented in Fig. 4.

In the first step of this flow chart, all the known data are loaded into the program. Then the salt gradient is set at the highest value (C_5-C_1). In the 3rd step of this program, the

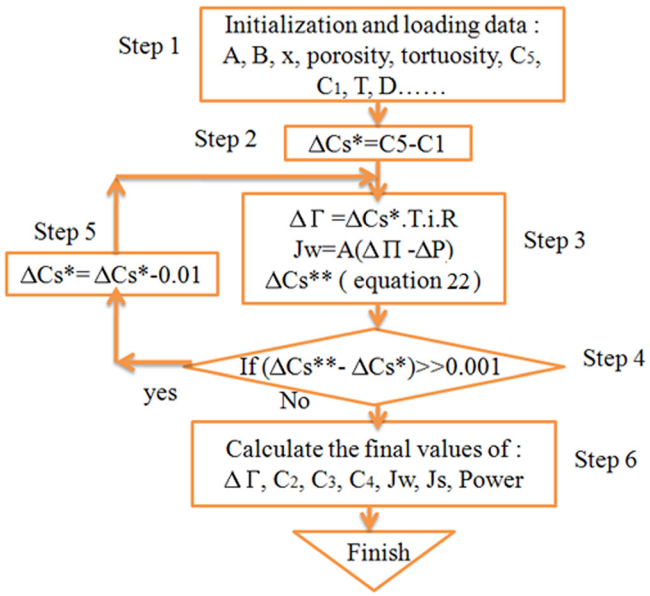

FIG. 4. Flow chart of the program used to solve the concentration equation.

TABLE I. Comparison of the model results with some published experiments. Adapted from Refs. 26 and 27.

References	A	B	S	C	ΔΓ (atm)			ΔP (atm)		Jw (μm/s)			Ws (W/m^2)		
	Related equation				Equation (5) where ΔCs is calculated from Eq. (13) (Fig. 4)			ΔP = ΔΓ/2		Equation (6)			Equation (7)		
Unit	m/s/Pa	m/s	mm	g/l	exp	mod	err (%)	exp	mod	err (%)	exp	mod	err (%)	exp	mod	err (%)
26	2×10^{-12}	6×10^{-8}	1	23.5	16	**15.7**	2	8	**7.85**	2	2.2	**2.1**	5	1.6	**1.65**	3
	7.1×10^{-12}	1.1×10^{-7}	0.67	26.9	21.5	**22**	2	10.8	**10.9**	1	2.5	**2.38**	5	2.7	**2.6**	4
27	1.87×10^{-12}	1.14×10^{-7}	0.68	35	27.6	**29**	5	9.7	**9.77**	1	2.81	**2.7**	4	2.73	**2.63**	4
	1.87×10^{-12}	1.14×10^{-7}	0.68	60	48.8	**50**	2	9.7	**9.6**	1	5.21	**5.2**	0.2	5.06	**4.99**	1

osmotic pressure is calculated by Van't Hoff law (5). This pressure is used to determine the water flux (6) and this value is then used to determine the new salt gradient using Eq. (22). The salt gradient values are compared in step 4; if the difference in these values is very high, the salt gradient is reduced in the 5th step, and else the program should exit from the loop in step 6.

5. Modeling results and model validation

A comparison between modeling results and experiments is required in order to validate the proposed model. Table I represents water flow, osmotic pressure, and specific power comparison between experimental results published in Refs. 26 and 27 and the model results. Two types of membrane have been tested in Ref. 26: asymmetric cellulose acetate (CA) membrane and TFC membrane. The CA membrane has a water permeate coefficient of 2×10^{-12} m/Pa/s and salt permeate coefficient of 6×10^{-8} m/s and structure parameter of 1 mm. This membrane has been tested with a NaCl solution having a concentration of 23.5 g/l. The measured osmotic power, water flow, and specific power are 16 atm, 2.2 μm/s, and 1.6 W/m^2, while the modeled ones are 15.7 atm, 2.1 μm/s, and 1.65 W/m^2 respectively.

Fig. 5 shows a comparison of the modeled results and experimental data published in Ref. 26 of the water flow and the specific power as a function of the hydraulic pressure. It can be seen that both the water flow and the specific power are almost the same for the experimental data and the model results. Also, it can be remarked that the maximum specific power is given for a hydraulic pressure equal to the half of the osmotic pressure.

The TFC membrane has been tested with a solution of 26.9 g/l of NaCl concentration. The comparison between the measured osmotic pressure and water flow with the modelled ones gives errors of 2.3% and 4.8%, respectively.

Another type of membrane called cellulose triacetate (CTA) has been experimentally tested in Ref. 27. This membrane was tested with NaCl solution with several concentrations. The values of water permeate coefficient, salt permeate coefficient, and the structure parameter were determined experimentally by reverse osmosis and forward osmosis. The comparison between experiment and modeling results for concentrations of 35 g/l and 60 g/l is represented in Table I. This comparison has errors between 1% and 5% on the osmotic pressure and water flow.

The correlation between these published experimental data and the model results indicate that the proposed model can be used as a tool to estimate the hydro-chemical parameters of a PRO plant.

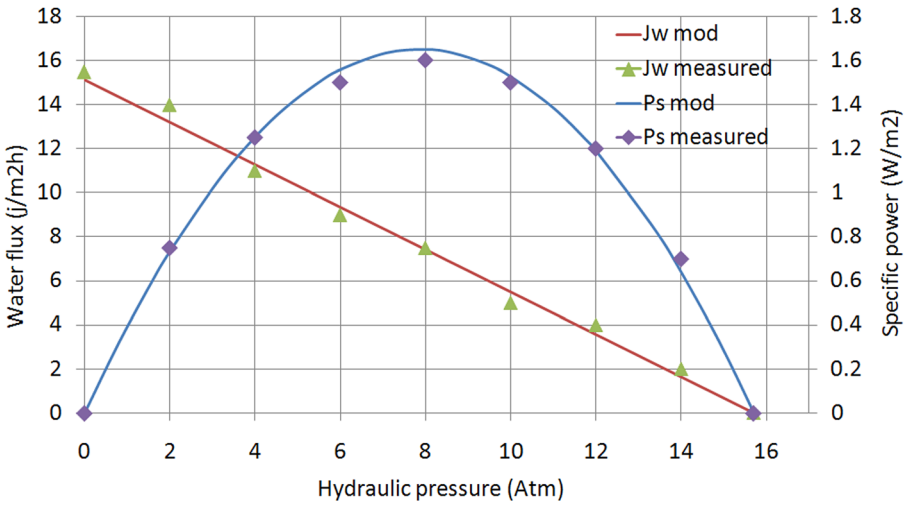

FIG. 5. Comparison of the modeled water flow and specific power results and experiments published in Ref. 26. Reprinted with permission from T. Thorson and T. Holt, J. Membr. Sci. **335**, 103 (2009). Copyright 2009 Elsevier.

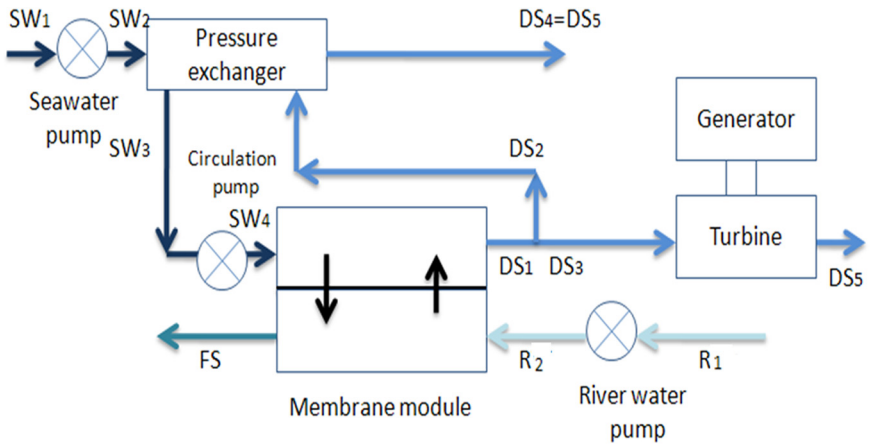

FIG. 6. Schematic of PRO technology used to determine the energy balance.

B. Energy balance of PRO system

To determine the energy balance, it is necessary to know the membrane characteristics (permeation to water, permeation to salt and structure). Also, it is required to determine the hydro-chemical parameters (flow rate, osmotic pressure, hydraulic pressure, and salt concentration) of the system in each of its points. These points are shown in Fig. 6; the abbreviations R, SW, FS, DS, and PW mean river water, seawater, flushing solution, diluted seawater, and permeated water, respectively.

Table I represents an example data for a river of 10 m^3/s of flow rate. This river has zero salinity and 10 °C of temperature and it flows in a sea having 30 PSU of salinity. About 80% of the fresh water flows through the membrane in order to avoid the membrane fouling.[25,27,28] The pressure losses of each pump and membrane module are equal to 0.2 atm. The efficiency of pumps, turbine, and generators is 86% each.

Table II represents the data and the formulas of the flow rate and the hydraulic pressure at different points of the whole system. The power generated by the turbine is given as

TABLE II. Example of necessary parameter for power calculation of pro plant.

	Parameter	Unit	Value
Environmental Conditions	River flow rate (R) (assumed)	m^3/s	10
	River sail concentration (C_1) (assumed)	PSU	0
	Process (water) temperature (T) (assumed)	°C	10
	Seawater salt concentration (C_5) (assumed)	PSU	30
Membrane proprieties and operating conditions	Water permeate coefficient (A) (datasheet)	m/s Pa	10^{-11}
	Membrane salt permeate coefficient (B) (datasheet)	m/s	3×10^{-8}
	Membrane structure parameter (S) (datasheet)	mm	0.3
	Film thickness (Δs and Δf) (estimated)	μm	25
	Fresh water utilization (c) (optimum operating point)	%	80
	SW/RW ratio (d)(assumed)		1.6
Equipments proprieties	Operating pressure ($P_{op} = \Delta\Gamma/2$) (our model)	kPa	791
	Module pressure losses (P_M) (datasheet)	kPa	20
	Pump pressure losses (P_R, P_{sw}, and P_{DS}) (datasheet)	kPa	20 (ea.)
	Pumps efficiencies (η_{RW}, η_{sw}, and η_{DS}) (datasheet)	%	96, 86, and 86
	Turbine and generator efficiencies (η_T, η_G)	%	86

TABLE III. Table of energy balance of the overall system.

Equipment	Flow rate (m^3/s)	Input pressure (kPa)	Output pressure (kPa)	η (%)	Power (kW)
River pump	10	101	121	86	233
Seawwater pump	16	101	121	86	372
Circulation pump	16	912	932	86	372
Pressure exchanger SW_2-SW_3	16	121	912		12 656
Pressure exchanger DS_2-DS_4	16	912	101	97	−12 656
Energy produced by turbine	8	101	912	86	−5580
Energy produced by generator				86	−4799
Net power					**−3822**

$$W_T = \eta_T \cdot Q_{DS3} \cdot (P_{DS3} - P_{DS5}), \tag{23}$$

where Q_{DS3}, P_{DS3}, and P_{DS5} are the flow rate at the point DS_3, the pressure at the point DS_3, and the pressure at the point DS_5 respectively

$$W_T = \eta_T \cdot \frac{(c+d)}{3} \cdot R \cdot (P_R + P_{op} + P_{DS} - P_M). \tag{24}$$

In this equation, P_{op} represents the half of osmotic pressure given by the model presented above; in this case, it is equal to 1582 kPa/2, which is low when compared to the ideal case (2300 kPa/2). R is the river flow rate.

The electrical power generated by the generator is given as

$$W_G = \eta_G \cdot W_T. \tag{25}$$

From Table III, the net power can be given as the difference in the generated power and the losses

$$W_{net} = W_G - \sum_{1}^{n} Q_i \cdot \Delta P_i. \tag{26}$$

In this equation, ΔP_i is the hydraulic pressure between the input and output of the equipment "i," Q is the flow in such equipment.

Table IV represents the estimated power generated by osmosis corresponding to the data of Tables I and II. The net power is calculated from Eq. (26); it can be seen that the net power

TABLE IV. Flow rate and hydraulic pressure at different points of the system.

Point	R_1	R_2	FS	SW_1	SW_2	SW_3
Flow rate (m^3/s)	R	R	R·(l-c)	R·d	R·d	R·d
Numerical values	10	10	2	16	16	16
Pressure (kPa)	P_1	P_1+P_R	P_1	P_1	$P_1 + P_{SW}$	$P_1 + P_{Rw}+P_{op}$
Numerical values	101	121	101	101	121	912
Point	S_4	DS_1	DS_2	DS_3	DS_4	DS_5
Flow rate (m^3/s)	R·d	R·(c+d)	R·(c+d)·2/3	R·(c+d)·l/3	R·(c+d)·2/3	R·(c+d)·l/3
Numerical values	16	24	14	8	16	24
Pressure (kPa)	P_1+P_R $+P_{op}+P_{DS}$	P_1+P_R $+P_{op}+P_{DS}$-P_M	$P_1+P_R+P_{op}$ $+P_{DS}$-P_M	$P_1+P_R+P_{op}$ $+P_{DS}$-P_M	P_1	P_1
Numerical values	932	912	912	912	101	101

produced by osmosis is 3822 kW for a river flow rate of 10 m^3/s and the power losses in the process is equal to 977 kW that represents about 24% of the generated power. This degradation in performance is mainly due to the membrane polarization and to the power consumed by the system equipment. This energy balance calculation will be used in Sec. II C to determine the potential of osmotic power in Quebec.

C. Application: Quebec

Geographically, the only contact of the province of Québec with the Ocean is either through James Bay (and the south of Hudson Bay) or the Saint Lawrence Gulf which is connected to the Great Lakes by the Saint Lawrence River.

The salinity of Bay of James is very low (less than 20 PSU) which makes the salinity power potential in this area uneconomical. Many freshwater rivers flow into the saline areas of the St. Lawrence, such as the rivers of Rimouski, Gaspé, and Sept-îles. The salinity gradient between these rivers can be exploited to produce clean energy.

Fig. 7 shows 16 rivers that have been selected in different areas of Quebec. Knowing the physical parameters of these rivers (Flow rate, temperature) and the saline area (the St. Lawrence Gulf salinity or the James Bay salinity), it is possible to determine the estimated power that can be produced in each intersection between the river mouth and saline area.

1. Salinity, temperature, and river flow rate distribution

All the rivers of Quebec that inflow into the saline area are situated in three watersheds: drainage basin Nr.7 (1–4 and 7–13), of the St. Lawrence North East Nr.2 (5, 6, and 14) of the St. Lawrence southeast, and the drainage basin Nr.9 (15 and 16) of the bays of James and Hudson.

The salinity and the temperature at the surface (3 m of depth) of the saline area close to these rivers are measured by the St. Lawrence Global Observatory; however, the river flow rate is measured by Centre d'Expertise Hydrique du Quebec.

FIG. 7. The selected rivers distributed in three watersheds in Québec.

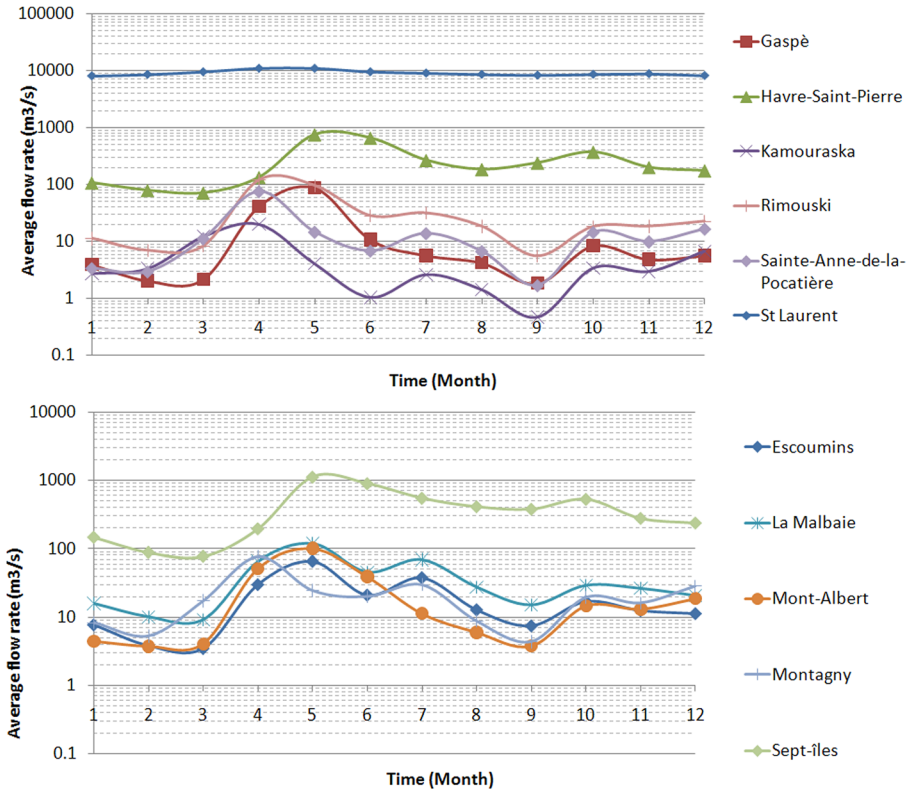

FIG. 8. Variation of the average flow rate of some rivers during the year.

Fig. 8 represents the variation of the average flow rate in the logarithmic scale of each river during the year. Here, the rivers in the north-west (Sept-îles and Harve Saint Pierre) have flows more than 10 times the other rivers. Moreover, the flow of each river in summer is about ten times higher than in winter.

The variation of the salinity and the temperature on the St. Lawrence in each area is presented in Figs. 9 and 10, respectively.

Fig. 9 shows the variation of the temperature at the surface during the year. The temperature at each point is very high in August; however, it is almost zero in four months (December, January, February, and March).

Fig. 10 shows that the salinity is divided into three areas: salinity very low in the south (Montagny), high salinity (15–25) up to La Malbaie, and ocean salinity after Les Escoumins (25–32). It can also be observed that the salinity at the surface in winter is little bit higher than in summer.

2. Annual power production by PRO and Hydro-Quebec comparison

Knowing the distribution of these parameters, it is possible to determine the estimated power produced by osmosis using Eq. (26) assuming a PRO plant with the same parameters as presented in Table I.

Figs. 11 and 12 show, respectively, the monthly and the yearly estimated average power produced by osmosis in some river mouths. In these graphs, the osmotic power in each river is very high in summer (May) when the river flow rates are maximum. In the winter, when both flow rate and temperature decrease, the potential of osmotic power will be about 10 times lower than in summer. It can be also seen that the potential in the Saint Lawrence (point Nr.1 of Fig. 7) represents the highest potential (about 1000 MW in summer).

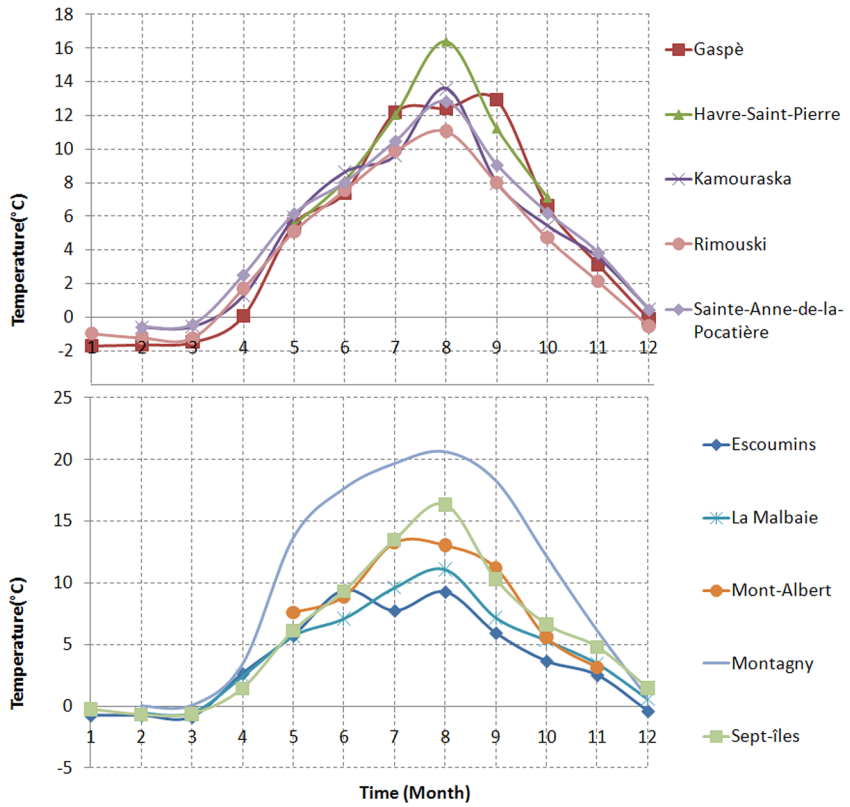

FIG. 9. The yearly distribution of the temperature at the surface of the St. Lawrence at different river mouths.

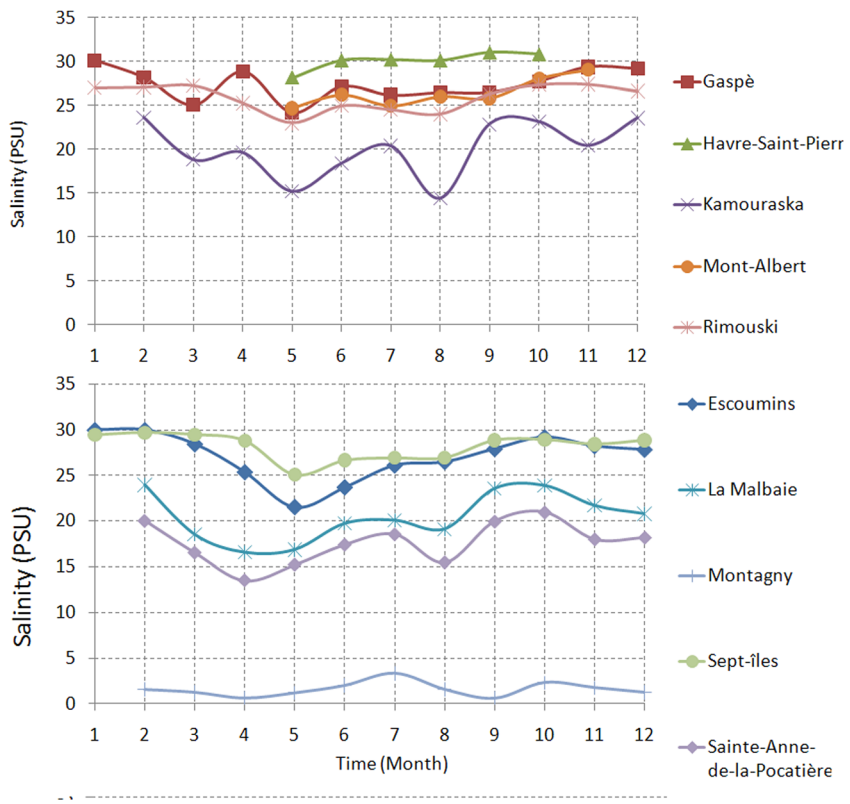

FIG. 10. The yearly distribution of the salinity at the surface of the St. Lawrence at different river mouths.

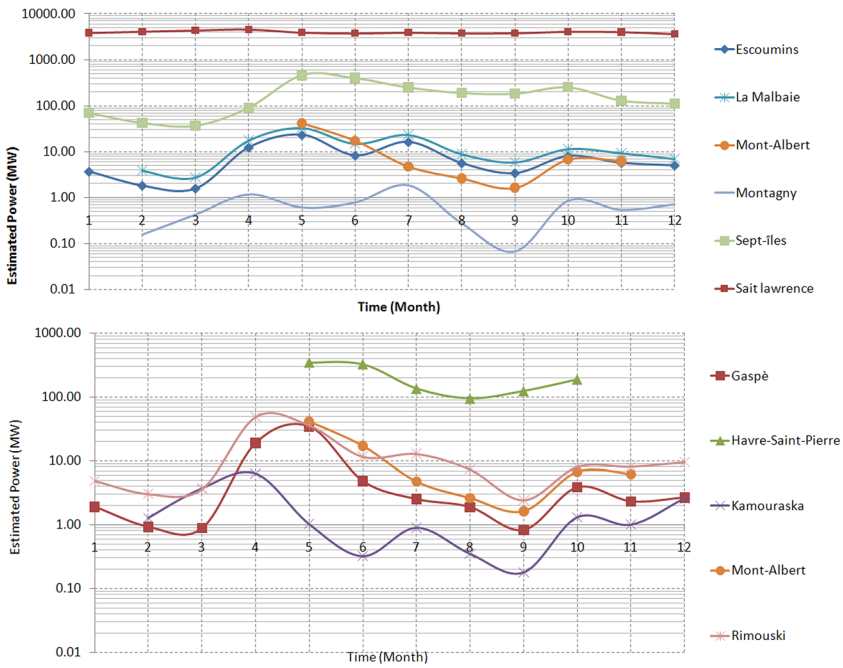

FIG. 11. The monthly average of the estimated produced power by osmosis in some river mouths of Quebec.

Fig. 13 shows a comparison between the produced energy by Hydro-Québec, the energy demand, and the estimated osmotic power. Here, the osmotic energy represents about 31% of the total electrical energy produced in Québec in summer and 17% in winter. The variation in the produced energy (and the demand) between the summer and the winter is about 35%; however, it is 11% for the estimated osmotic power. But, the estimated osmotic power potential is about 10 times higher than all the current renewable energy sources in Québec (Thermal, nuclear, gas turbine, and wind).

3. Osmotic power production based on minimum flow rate

The minimum flow rate of some rivers can reach zero. To make the study more significant, the osmotic power potential should be calculated based on the minimum flow rate. Table V shows the estimated salinity power potential in Quebec based on the minimum flow rate in all the selected points (Fig. 7). This table illustrates that the osmotic power can be mostly produced from the St. Lawrence itself at the point where it becomes increasingly salty at the head

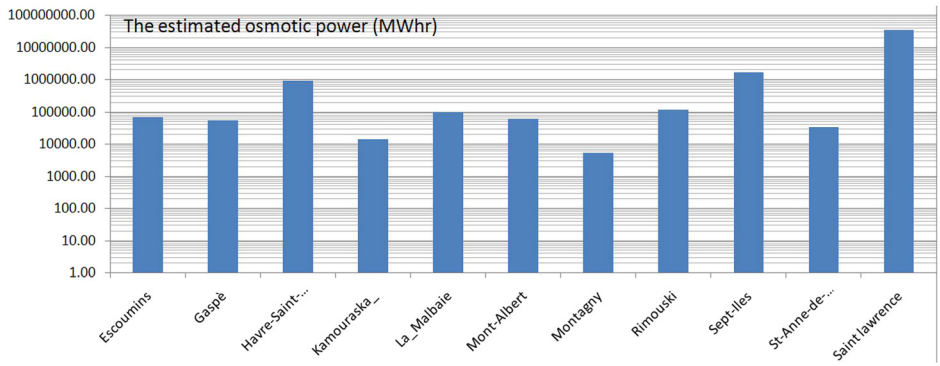

FIG. 12. The yearly energy of the estimated produced power by osmosis in some river mouths of Quebec.

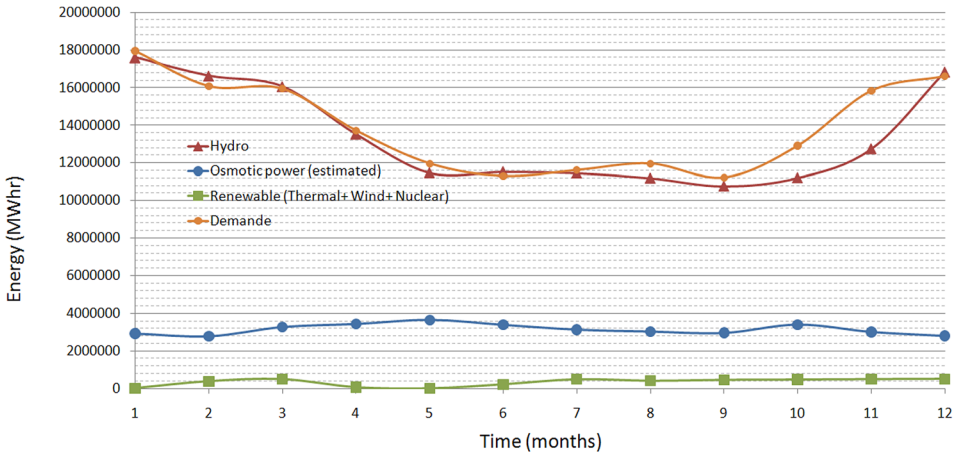

FIG. 13. Comparison between the produced energy by Hydro-Québec and the estimated osmotic power.

of the Laurentian Channel (point Nr.1) with a potential of 3975 MW. Then, the rivers situated in the drainage basin Nr.7 represent the highest osmotic power potential because of their high flow rate and their inflow in a very saline area. However, the potential is very low in the drainage basin Nr.9 and Nr.2, because of their low salinity and low flow rate respectively.

The osmotic power potential that can be produced in the 7th drainage basin is estimated at 5108 MW making a total annual energy of 44.57 TWh/yr that represents 27% of the total energy produced by Hydro-Quebec in 2009.[7]

TABLE V. The estimated osmotic power based on minimum flow rate.

					Without polarization		With polarization	
Station	River	Coordinate	Q average (m^3/s)	Q min (m^3/s)	Turbine power (MW)	Net power (MW)	Turbine power (MW)	Net power (MW)
1	Sait Laurent	47°59′N, 69°45′W	12 500	8000	6720.88	5724.14	4744.24	4024.24
2	Nétagamiou	50°42′N, 59°35′W	501	162	133.24	113.46	93.28	79.09
3	Saguenay	48°07′N, 69°42′W	1 750	1000	825.66	703.09	578.58	490.60
4	Manicouagan	49°11′N, 68°18′W	560	560	461.86	393.29	323.50	274.30
5	Matane	48°50′N, 67°31′W	46	46	37.51	31.94	26.26	22.26
6	Gaspe	48°58′N, 64°41′W	17	3	2.19	1.86	1.53	1.30
7	Petit mecatina	51°12′N, 58°35′W	206	46	37.99	32.35	26.59	22.55
8	Moisie	50°12′N, 66°05′W	413	92	75.90	64.63	53.14	45.05
9	Aux outrardes	49°04′N, 68°25′W	400	100	82.38	70.15	57.67	48.90
10	Betsiamites	48°55′N, 68°38′W	340	110	90.62	77.17	63.44	53.79
11	Romaine	50°17′N, 63°48′W	292	69	56.84	48.40	39.79	33.74
12	Natashquan	50°08′N, 61°37′W	366	98	81.02	68.99	56.72	48.09
13	Sainte Marguerite	50°09′N, 66°36′W	100	40	32.95	28.06	23.06	19.56
14	Rimouski	48°24′N, 68°33′W	25	6	5.16	4.40	3.61	3.06
15	Pontax	51°32′N, 78°5′W	102	21	11.53	9.77	8.07	6.80
16	Rivière de la Baleine	55°14′N, 76°59′W	542	149	81.86	69.36	57.31	48.25
Total					**8738**	**7441**	**6157**	**5222**
Total (energy) (TWh)					**75.33**	**64.16**	**53.09**	**45.03**

Fig. 7 shows that a big part of Hydro-Quebec electrical grid is situated in the 7th drainage basin which is considered another advantage because it makes the connection of future osmotic plants to the grid easier and economical.

III. CONCLUSION

In this paper, the principle, advantages, and development trends of the most advanced technologies (PRO and RED) which are used to exploit power from the salinity gradient are discussed.

A modeling approach of membrane polarization has been performed and validated. An osmotic energy balance study has been carried out in order to estimate the energy produced from gradients in salinity, using PRO technology.

This energy balance has been applied to many rivers located in different areas of Quebec, merging in the saline area (the St. Lawrence Gulf or James Bay). The results show that the osmotic power potential is low in the southeast of the St. Lawrence due to the low rivers flow rate and in the bays of James and Hudson due to their low salinities. However, it is very high in the north-east of the St. Lawrence where this can go up to 45 TWh of power, representing more than 27% of the total energy produced by Hydro-Quebec in 2009. Furthermore, having the largest part of conventional electrical grid in this drainage basin is another advantage.

ACKNOWLEDGMENTS

Thanks to Claude B. Laflamme, Amer Alghabra, Lafleur Caroline, Diane Morin, and Maged Barsom from l'IREQ, Hydro-Québec, Institut Maurice-Lamontagn, Centre d'expertise hydrique du Québec and Concordia for their help and assistance to write this paper.

NOMENCLATURE

A	water permeate flux coefficient (m s^{-1} Pa)
B	Salt permeate coefficient (m s^{-1})
C	salt concentration (mol l^{-1})
c	amount of the freshwater utilized by the membrane (%)
C_1	salt concentration of the river (mol l^{-1})
C_2	salt concentration on the surface of the porous support (mol l^{-1})
C_3	salt concentration on the membrane surface in the freshwater side (mol l^{-1})
C_4	salt concentration on the membrane surface in the seawater side (mol l^{-1})
C_5	salt concentration of the seawater (mol l^{-1})
ΔC_S	salt concentration difference between the membrane surfaces (mol l^{-1})
D	salt diffusion coefficient (m^2 s^{-1})
d	the Ratio between the freshwater and the seawater flows rate (%)
i	Van't Hoff coefficient (2 for NaCl)
J_w	water flux (m s^{-1})
Js	salt diffusive flux (mol M^{-2} s^{-1})
K_B	Boltzmann constant 1.38×10^{-23} m^2 kg s^{-2} K^{-1}
L	length of the porous material (m)
L_0	effective length of the porous material (m)
M_{NaCl}	molar mass (g mol^{-1})
P_M	pressure losses across the membrane module (Pa)
P_{op}	operating pressure ($\Delta\Gamma/2$) (Pa)
P_{SW}	pressure losses across the seawater pump (Pa)
P_{DS}	=pressure losses across the circulation pump (Pa)
ΔP	hydraulic pressure difference (Pa)
Q	water flow rate (m^3 s^{-1})
R_g	gas constant (8.314472 J·mol^{-1}·K^{-1})
R	is the river flow rate (m^3 s^{-1})

r	radius of the diffused particle (m)
S	porous structure parameter (m)
T	operating temperature (K)
t	the time (s)
V_P	water flux in the porous medium (m s^{-1})
$\vec{V}$	liquid velocity vector
Ws	specific power (W m^{-2})
W_T	the hydraulic power generated by the turbine (W)
W_{net}	net power (W)
W_G	the electrical power generated by the generator (W)
$\Delta\Gamma$	the osmotic pressure difference (Pa)
μ	liquid viscosity (Pa s)
Δf	fresh water side film thickness (m)
Δs	seawater side film thickness (m)
Ψ	porosity of the porous material
τ	tortuosity of the porous material
η_R	efficiency of the river water pump
η_{SW}	efficiency of the seawater pump
η_{DS}	efficiency of the circulation pump
η_G	efficiency of the generator (%)
η_T	efficiency of the turbine (%)

Abbreviations

R	river water
SW	seawater
FS	flushing solution
DS	diluted seawater
PW	permeated water

[1]See www.mddep.gouv.qc.ca for Quebec Action Plan on Climate Change (QAPCC), Government of Quebec (2008).
[2]G. L. Wick and W. R. Schmitt, "Prospects for renewable energy from the sea," Mar. Technol. Soc. J. **11**, 16–21 (1977).
[3]J. W. Post *et al*., "Salinity-gradient power: Evaluation of pressure-retarded osmosis and reverse electrodialysis," J. Membr. Sci. **288**, 218–230 (2007).
[4]G. Alstot *et al*., "Hydrocratic generator," U.S. patent 0,116,689 (22 May 2008).
[5]R. J. Seymour and P. Lowrey, "State of the art in other energy sources," in *Ocean Energy Recovery: The State of the Art*, edited by R. J. Seymour (ASCE, 1997), pp. 258–275.
[6]S. Loab, "Method and apparatus for generating power utilizing pressure-retarded-osmosis," U.S. patent 3,906,250 (28 June 1971).
[7]S. Loeb, "Effect of porous support fabric on osmosis through a Loeb-Sourirajan type asymmetric membrane," J. Membr. Sci. **129**, 243–249 (1997).
[8]S. Loeb, "Energy production at the Dead Sea by pressure-retarded osmosis: Challenge or chimera?," Desalination **120**, 247–262 (1998).
[9]S. Loeb, "One hundred and thirty benign and renewable megawatts from Great Salt Lake? The possibilities of hydroelectric power by pressure-retarded osmosis," Desalination **141**, 85–91 (2001).
[10]S. E. Skilhagen, J. E. Dugstadand, and R. J. Aaberg, "Osmotic power production based on the osmotic pressure difference between waters with varying salt gradients," Desalination **220**, 1–3 (2008).
[11]T. Thorsen and T. Holt, "Semi-permeable membrane, method for providing electric power and device," International patent (PCT) 02/13955 (15 August 2001).
[12]T. Thorsen and T. Holt, "A method and a system for performing maintenance on a membrane used for pressure retarded osmosis," International patent (PCT) WO 073207 (13 September 2001).
[13]See www.statkraft.com for StatKraft Annual Report (2009).
[14]J. Veerman *et al*., "Reducing power losses caused by ionic shortcut currents in reverse electrodialysis stacks by a validated model," J. Membr. Sci. **310**, 418–430 (2008).
[15]P. Długołecki *et al*., "Current status of ion exchange membranes for power generation from salinity gradients," J. Membr. Sci. **319**, 214–222 (2008).
[16]P. Długołecki *et al*., "Transport limitations in ion exchange membranes at low salt concentrations," J. Membr. Sci. **346**, 163–171 (2010).
[17]P. Długołecki *et al*., "On the resistances of membrane, diffusion boundary layer and double layer in ion exchange membrane transport," J. Membr. Sci. **349**, 369–379 (2010).

[18]Y. Berrouche, *L'Electro-Osmose Dans Les Milieux Poreux: Théorie, Modélisation, Conception et Application au Refroidissement Passif des Composants de Puissance* (EUP, 2010), pp. 20–25.
[19]J. Veerman *et al*., "Electrical power from sea and river water by reverse electrodialysis: A first step from the laboratory to a real power plant," Environ. Sci. Technol. **44**, 9207–9212 (2010).
[20]See www.wetsus.nl for Wetsus website.
[21]See www.mddep.gouv.qc.ca for Ministère du Développement durable de l'Environnement, des Parcs de Quebec.
[22]U.S. Department of Energy, *Handbooks of Methods for the Analysis of the Various Parameters of the Carbon Dioxide System in Seawater*, Version 2 (US DOE, 1994), Chap. 5.
[23]F. J. Millero and W. H. Leung, "The thermodynamics of seawater at one atmosphere," Am. J. Sci. **276**, 1035–1077 (1976).
[24]A. Einstein, "Über die von der molekularkinetischen Theorie der Wärme geforderte Bewegung von in ruhenden Flüssigkeiten suspendierten Teilchen," Ann. Phys. **322**(8), 549–560 (1905).
[25]T. Thorsen and T. Holt, "Semi-permeable membrane, method for providing electric power and device," International patent WO 02/13955 A1 (2002), pp. 29.
[26]T. Thorson and T. Holt, "The potential for power production from salinity gradients by pressure retarded osmosis," J. Membr. Sci. **335**, 103–110 (2009).
[27]A. Achillia, T. Y. Cathb, and E. Amy, "Power generation with pressure retarded osmosis: An experimental and theoretical investigation," J. Membr. Sci. **343**, 42–52 (2009).
[28]See www.hydroquebec.com for Hydro-Quebec, 2009 rapport annuel: l'energie de notre avenir.